

# Dynamics and stability of U(1) spin liquids beyond mean-field theory

Josef Willsher<sup>1,2,\*</sup> and Johannes Knolle<sup>1,2,3</sup>

<sup>1</sup>Technical University of Munich, TUM School of Natural Sciences, Physics Department, 85748 Garching, Germany

<sup>2</sup>Munich Center for Quantum Science and Technology (MCQST), Schellingstr. 4, 80799 München, Germany

<sup>3</sup>Blackett Laboratory, Imperial College London, London SW7 2AZ, United Kingdom

(Dated: March 19, 2025)

Quantum spin liquids (QSLs) are long-range entangled phases of frustrated magnets exhibiting fractionalized spin excitations. In two dimensions, there is limited analytical understanding of their excitation spectra beyond parton mean-field theories, which fail to capture many features of the finite frequency dynamical response from recent experimental and numerical works. We use a self-consistent random phase approximation (RPA) for the  $J_1$ - $J_2$  Heisenberg model on the triangular lattice to describe the strong spinon-spinon interactions of the U(1) Dirac QSL. We obtain quantitative results for the dynamical spin structure factor and phase diagram compatible with comprehensive numerical efforts. We extend the method to chiral QSLs, and discuss its broad range of applicability to other models and for describing inelastic neutron scattering experiments.

*Introduction.* Quantum spin liquids (QSLs) are spin-disordered phases of frustrated magnets which are characterized by their *emergent gauge structure*, long-range entangled ground states and unconventional fractionalised excitations. This includes spinons, fermionic particles carrying half the spin flip quantum number of a magnon [1–4]. Aside from rare fine-tuned exactly soluble examples [5], QSLs are generally strongly interacting quantum many-body systems whose low energy description is believed to be described by lattice gauge theories — an imposing theoretical challenge. Our understanding of these models is therefore limited to approximate descriptions [1, 2, 6, 7]. Parton mean-field theories (MFTs) are successful at classifying the zoo of QSLs, which cannot be categorized within the symmetry-based Landau paradigm, and tell us the leading-order excitations.

Parton MFTs are also the starting point for analyzing the stability of QSL states with respect to asymptotic long wavelength fluctuations of the gauge field. However, in general they are uncontrolled approximations which fail to capture many important features in the non-universal, finite-frequency response functions. In this Letter, we extend parton MFT to include fluctuations of the QSL and competing spin order parameters, which allows us to extract quantitative predictions for phase diagrams of spin models and make connections to inelastic scattering experiments of recent candidate materials. To this end, we focus on the exchange-frustrated spin-half Heisenberg model on the triangular lattice,

$$\mathcal{H}_{J_1 J_2} = \sum_{\langle ij \rangle} J_{ij} \vec{S}_i \cdot \vec{S}_j, \quad (1)$$

where  $J_{ij}$  is  $J_1$  on nearest-neighbor bonds and  $J_2$  on next-nearest, shown in Fig. 1(a). In the semiclassical description the model has a transition between 120-degree and stripe magnetic order at  $J_2/J_1 = 1/8$  [8, 9], Fig. 1(b). Numerical results for the quantum spin-half model find strong evidence for a critical QSL separating the ordered phases [10–16], Fig. 1(d,e).

A common starting point for analytical treatment is a transformation into the Abrikosov (fermionic parton) representation  $\vec{S}_i = \frac{1}{2} f_{i,\alpha}^\dagger \vec{\sigma}_{\alpha\beta} f_{i,\beta}$  and the resulting interacting theory reads

$$\mathcal{H} = -\frac{1}{2} \sum_{ij} J_{ij} \left( f_{i\alpha}^\dagger f_{j\alpha} f_{j\beta}^\dagger f_{i\beta} + \frac{1}{2} f_{i\alpha}^\dagger f_{i\alpha} f_{j\beta}^\dagger f_{j\beta} \right). \quad (2)$$

The physical Hilbert space must be projected out by requiring one fermion per site, via  $f_{i\alpha}^\dagger f_{i\alpha} = 1$ . The model with interactions and filling constraint is analytically intractable. One then describes the low-energy spectrum of the emergent QSL phase by resorting to MFT [1, 2]. However, this approach alone has fundamental limitations: it gives a wrong account of high-energy excitations, which actually dominate the spectral response, and the stability of the QSL phase is grossly overestimated. For example, a nearest-neighbor Dirac QSL Ansatz on the triangular lattice is completely agnostic to the  $J_2$  interaction strength which we know (only from numerics) is needed to stabilize the QSL, see Fig. 1(d,e).

As our main result, we calculate the dynamical spin structure factor within a self-consistent MFT+RPA theory without free parameters. We find that in addition to spinon continua a new sharp mode dominates the finite-frequency response, which can be thought of as a *spinon exciton* bound state induced by the interactions. Moreover, by tuning the ratio  $J_2/J_1$  the sharp mode condenses at high symmetry points of the Brillouin zone, indicating instabilities of the QSL to nearby ordered phases. The resulting phase diagram and dynamical structure factor are in remarkable agreement with state-of-the-art numerical calculations for the model's ground state [11, 13, 16] and time-dependent response [15–17].

*Parton MFT and Fluctuations.* We decouple the quartic interaction, Eq. 2, with the bond-singlet parameter  $t_{ij} = J_{ij} \langle f_{i\alpha}^\dagger f_{j\alpha} \rangle$  and enforce the constraint on av-

erage  $\langle f_{i\alpha}^\dagger f_{i\alpha} \rangle = 1$ . The mean-field Hamiltonian is

$$\mathcal{H}_0 = \sum_{ij} t_{ij} f_{j\alpha}^\dagger f_{i\alpha} + \text{h.c.} \quad (3)$$

with complex nearest-neighbor hoppings with uniform amplitude, which we write as  $t_{ij} = te^{ia_{ij}}$ . We focus on the U(1) Dirac spin liquid in this work, formed by a staggered  $[0, \pi]$  flux Ansatz  $t_{ij} = \pm t$  with alternating fluxes through adjacent triangular plaquettes, see Fig. 1(a), which has been shown to be the lowest energy Ansatz in variational Monte Carlo (VMC) [13]. The resulting free fermion theory has  $N_f = 4$  Dirac cones in the first Brillouin zone but neglects fluctuations of the gauge field and interactions between fermions.

The model has a U(1) gauge redundancy  $f_{i\alpha}^\dagger \rightarrow e^{i\theta_i} f_{i\alpha}^\dagger$  and  $a_{ij} \rightarrow a_{ij} - \theta_i + \theta_j$ , which implies that the gauge excitations are gapless. In the parlance of Ref.[7], ‘first-order’ MFT accounts for the effect of these gapless transverse (phase) fluctuations of the singlet order parameters on the stability of the QSL Ansatz. For the case of U(1) Dirac QSLs the most relevant gauge field fluctuations are monopole instanton events, which tunnel  $2\pi$  emergent flux [18]. The symmetry properties of these monopoles, and hence the fate of the phase, is highly lattice-dependent; in the case of the triangular lattice, no relevant monopoles exist which are singlets under the lattice symmetry group, and so the QSL is stable [19, 20]. Furthermore, strong-coupling results imply that the spin susceptibility diverges at low energies about the corners of the Brillouin zone  $\mathbf{K}$ , as  $S(\mathbf{K}, \omega) \sim \omega^{-(3-2\Delta_\Phi)}$  where  $\Delta_\Phi$  is the scaling dimension of the monopole [21, 22]. We stress, however, that this monopole continuum is only the expected limiting response at lowest energies, and for a given lattice model the scale below which it appears can be small. Thus, it may not describe the dominant non-universal response at higher energy as relevant for experiments and finite size numerics.

Beyond first-order MFT, we must investigate *amplitude fluctuations* in addition to the transverse phase fluctuations. The MFT order is characterized by a finite uniform amplitude of  $t = J_1 |\langle f_i^\dagger f_j \rangle|$ , as well as a constant (zero) spin order  $m_i^\alpha = \frac{1}{2} \langle f_i^\dagger \sigma^\alpha f_i \rangle = 0$ . Fluctuations of these parameters lead to spin-0/1 collective modes which can dominate the high energy spectrum [23]. In the MFT treatment, these fluctuations are gapped and, therefore, may be neglected. However, we find that their condensation as a function of interaction strength leads to quantitative predictions for the phase boundaries of the QSL. Developed in detail in the next section, we will show that there is a sharp bosonic (spin-1) mode at low energy in the spin structure factor. Its minimum gap is at the  $\mathbf{K}$  point and varies as a function of  $J_2$ , plotted in Fig. 1(c). This excitation has a spin-flip quantum number and condenses at zero energy below  $J_{2c} = 0.0715$ , signaling a continuous transition to 120-degree magnetic order.

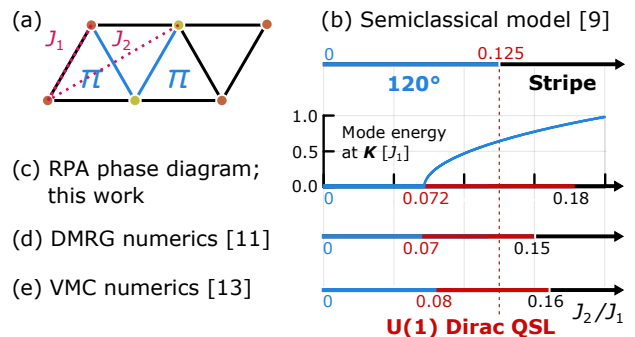


Figure 1. (a) Triangular lattice  $J_1$ - $J_2$  Heisenberg interactions along nearest and next-nearest neighbor bonds highlighted.  $\pi$ -flux Ansatz shown on a two-site unit cell; black/colored bonds have  $\pm$  sign in the Hamiltonian. (b) Semiclassical phase diagram of the model; first-order transition from 120-degree to stripe magnetic order at  $J_2/J_1 = 1/8$  [9]. (c) Phase diagram inferred from the stability of the U(1) Dirac QSL Ansatz beyond mean field theory. Inset figure shows the gap of spinon excitations at the  $\mathbf{K}$  point, as calculated in the RPA. (d,e) Comparison of the theoretical prediction with large-scale numerical results, using density-matrix renormalization group (DMRG) [11] and variational Monte Carlo (VMC) [13] methods.

*Dynamical Response.* Our main interest is the spin structure factor

$$S(\mathbf{q}, \omega) = \frac{1}{N} \sum_{ij} e^{-i\mathbf{q}\cdot(\mathbf{i}-\mathbf{j})} \int dt e^{i\omega t} \langle S_i^z(t) S_j^z(0) \rangle, \quad (4)$$

that is directly proportional to the cross section of inelastic neutron scattering (INS) experiments. We calculate the *spinon contribution* using the Abrikosov representation (details in the End Matter). It is related to the interacting susceptibility  $[\chi(\mathbf{q}, \omega)]_{XY}^{\alpha\beta}$  in the spin channel as

$$S(\mathbf{q}, \omega) = \text{Im} \sum_{X,Y=A,B} e^{-i\mathbf{q}\cdot(\mathbf{r}_X - \mathbf{r}_Y)} [\chi(\mathbf{q}, \omega)]_{XY}^{zz}. \quad (5)$$

Given the MFT Eq. (3), one can evaluate the free fermion-fermion susceptibility  $[\chi^0(\mathbf{q}, \omega)]_{XY}^{\alpha\beta}$  but it fails to describe the strongly interacting model of Eq. (2), e.g. there are no low-energy excitations around the  $\mathbf{K}$  momenta at all. We employ the RPA to treat the four-fermion interaction term (2), which consists of summing up an infinite series of bubble diagrams [24, 25].

Note that in itinerant *ordered* magnets described by Hubbard-like models similar self-consistent theories have successfully described the dynamical spin response and collective spin wave modes [26–30], including on the triangular lattice [31]. Previous applications within parton MFT treated an on-site Hubbard  $U$ , which approximately imposes the on-site single-filling constraint [32, 33] or arises due to screened gauge fluctuations in a magnetized QSL with a Fermi surface [34]. Here, we

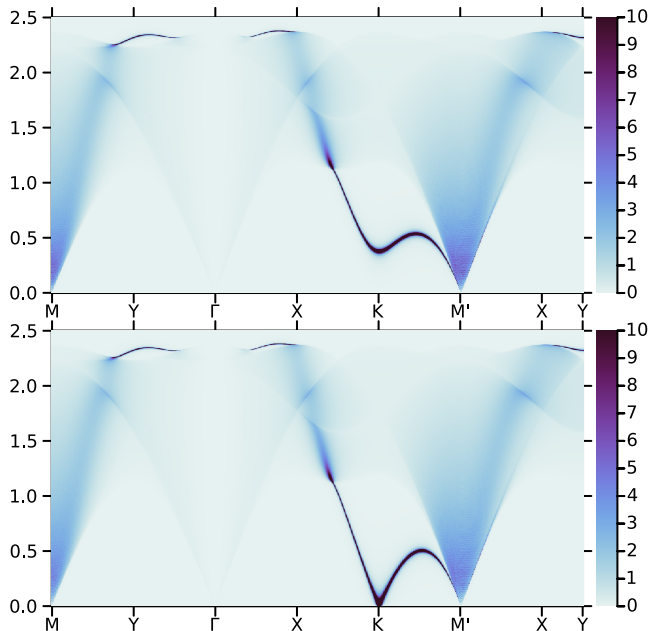


Figure 2. Fermion contribution to the dynamical structure factor  $S(\mathbf{q}, \omega)$  in the random phase approximation. We take  $J_2/J_1 = 0.09$  in the U(1) Dirac QSL phase (top) and  $J_{2,c}/J_1 = 0.0715$  at the transition to 120-degree order (bottom). All energies  $\omega$  in units of  $J_1$ .

consider only the effect of interactions  $[J(\mathbf{q})]_{XY}$  on dynamical response functions [35–37], given by the real-space nearest- and next-nearest-neighbor interaction  $J_{ij}$ , as Eq. (2). The RPA susceptibility matrix in terms of the interaction reads:

$$\hat{\chi}(\mathbf{q}, \omega) = \left[ 1 + 2\hat{J}(\mathbf{q}) \cdot \hat{\chi}^0(\mathbf{q}, \omega) \right]^{-1} \cdot \hat{\chi}^0(\mathbf{q}, \omega); \quad (6)$$

we emphasize that all quantities here are sublattice matrices, derived in the End Matter. The elements of the interaction matrix  $\hat{J}(\mathbf{q})$  are given by  $J_{1,2}$  and the bare  $\hat{\chi}^0$  is fixed by the MFT QSL order  $t/J_1 = |\langle f_{i\alpha}^\dagger f_{j\alpha} \rangle| = 0.395$ . The self-consistent nature means we can produce a *quantitative phase diagram* Fig. 1(c) as a function of the exchange interactions  $J_2/J_1$ . The spinon contribution to the dynamical structure factor is shown in Fig. 2 with  $J_2/J_1 = 0.09$  in the stable regime (upper panel) and with  $J_2/J_1 = 0.0715$  at the phase boundary to 120-degree order (lower panel).

*Spinon bound state.* The most striking effect of the spinon interactions is to create a sharp paramagnon mode coming down to low energy; this *spinon exciton*, a quasi-particle with quantum numbers of a magnon arising as a two-spinon bound state, displays a magnetoroton-like minimum around  $\mathbf{K}$ . It is a signature of the proximate 120-degree order distinct from the monopole continuum at the same wavevector. The mode broadens when entering the two-spinon continuum but exits above it around the  $\Gamma$  point, in remarkable agreement VMC results [15].

Overall, the spinon exciton dominates the response; the only broad continuum at low energies is present at the  $\mathbf{M}$  points from inter-Dirac cone transitions, but with weaker spectral weight in agreement with time-dependent DMRG results [16].

The gap  $m \approx 0.4J_1$  is at low energy relative to the magnetic exchange scale and tuning  $J_2 < J_{2c} = 0.0715 J_1$  leads to the gap closing  $m \rightarrow 0$ , shown in Fig. 1(c). After condensation, the paramagnons continuously become the Goldstone modes of the 120-degree magnetic order. At the  $\mathbf{M}$  point, the mode is also at low energies within the spinon continuum, leading to an enhancement of low-energy spectral weight relative to the free-fermion MFT case (c.f. Fig. 6 in End Matter). Tuning  $J_2 > 0.18 J_1$ , the pole of Eq. (6) also diverges at  $\mathbf{M}$  as  $\omega \rightarrow 0$ , signaling a tendency for stripe magnetic order. However, one needs to be cautious about this transition because the large spectral weight at low energies can cause a sooner first-order transition to stripe order (as reported consistently by numerical works around  $J_2 \approx 0.15 J_1$  [10–16]).

*Gauge fluctuations.* What is the effect of gauge field fluctuations on these predictions for the phase diagram and resulting spin-spin correlations? Let us recap the case of first-order MFT, where we include the effect of fermion-gauge coupling while ignoring fermion-fermion interactions. At low energies  $\omega \ll J_1$ , the only matter excitations are fermion bilinears of the Dirac cones. Writing fermions as spinor fields  $\psi_i$ , the fermion-gauge coupling can be written compactly as a gauge-covariant derivative in the effective action  $\mathcal{L}_{\text{QED}_3} = \sum_{i=1}^4 \bar{\psi}_i (\not{\partial} - i\not{a}) \psi_i$ . This emergent QED<sub>3</sub> is believed to flow to a strong-coupling conformal (CFT) fixed point, meaning there are no relevant symmetry-allowed gauge or fermion-fermion interactions [19, 20], and there is no spontaneous chiral symmetry breaking [38, 39]. The relevant spin-1 fluctuations of the gauge field at low energy are the gapless monopoles carrying momentum  $\mathbf{K}$  [19, 20, 40, 41].

Although four-fermion interactions  $(\bar{\psi}\vec{\sigma}\psi)^2$  are strictly irrelevant at the CFT fixed point [42], they are arbitrarily (non-perturbatively) large in the parent spin-Hamiltonian. Hence, they may anyway be able to drive a fermion-mass generation and phase transition to an ordered phase, or produce non-universal contributions to correlation functions. To understand this transition, one can decouple the four-fermion interaction using a Hubbard–Stratonovich transformation

$$\mathcal{L}_{J_1-J_2} = \sum_i \bar{\psi}_i (\not{\partial} - i\not{a} - \vec{\sigma} \cdot \vec{\varphi}) \psi_i + \frac{1}{2} m^2 |\vec{\varphi}|^2, \quad (7)$$

which results in a chiral-Heisenberg–Gross–Neveu (cHGN) coupling. We derive this continuum theory from (2) in the Supplementary Materials from our lattice scale calculation. The theory describes the QSL-ordered transition as  $m \rightarrow 0$ , where the fluctuations of the spin-order parameter  $\vec{\varphi}$  condense, gapping the spinons. The resulting ‘cHGN-QED<sub>3</sub>’ fixed point is marked by strong fluctu-

ations of both the gapless gauge field and a critical boson [43], the latter simply identified as our spinon exciton.

Far away from the transition to 120-degree order, the mode is gapped  $m \sim J_1$ . At lowest energies  $\omega \ll J_1$  the boson can be neglected, and so the structure factor at the monopole wavevector diverges as  $S(\mathbf{K}, \omega) \sim \omega^{-3+2\Delta_\Phi}$ . In the following, we take the large- $N_f$  value of the QED<sub>3</sub> monopole scaling dimension as  $\Delta_\Phi = 1.02$  [44]. Because of the complete separation of scales, the contribution of the paramagnon mode and monopoles separate; the total contribution (I) is shown in Fig. 3(a). The low-energy response is dominated by the monopole power law (dashed gray line), and the paramagnon appears as a sharp pole at high energy. Approaching the transition, the paramagnon mode lowers in energy entering the continuum of the monopole. The Hubbard–Stratonovich mode  $\varphi$  has identical quantum numbers to the spin-1 monopole  $\Phi$  [19, 20], leading to a hybridization of the two quasiparticles (similar to the hybridization of spin-0 monopoles and phonons recently discussed in Ref. [22]). In this regime (II), we perform a perturbative calculation to characterize the coupling of the paramagnon to the gauge field [45]. The combined structure factor is plotted in Fig. 3(c), showing a broadening of the paramagnon, with a slice also shown as line II in Fig. 3(a). Note, this perturbative approach breaks down as  $J_2 \rightarrow J_{2,c}$ , where the monopoles and paramagnons fully hybridize. At this new critical point, the SU(4) symmetry of QED<sub>3</sub> is broken, and the spin-1/0 monopoles are split, meaning the spin-structure factor is controlled by a shifted exponent  $\tilde{\Delta}_\Phi < \Delta_\Phi$ , which we take to be 0.78 (again from an appropriate large- $N_f$  calculation) [43]. Away from the exact critical point, we expect an appropriate scaling collapse in terms of  $\mathcal{G}(\omega/m)$ .

We may also evaluate the real-space spin-spin correlations  $g(r) = \langle \vec{S}_{r\mathbf{a}_2} \cdot \vec{S}_0 \rangle$  (in the direction of nearest-neighbor bonds  $\mathbf{a}_2$ ) within these three regimes, shown in Fig. 3(b). Away from the critical point (I,II) the long-distance behavior is dominated by a power-law tail, governed by the universal QED<sub>3</sub> monopole exponents  $g(r) \sim r^{-2\Delta_\Phi}$ , with a large non-universal correction at short distances  $r < \xi \approx 5$  due to the paramagnon at finite energies. Approaching the critical point, this correlation length will diverge  $\xi \sim m^{-1}$ , and the spin-spin correlations (marked III) will cross over to cHGN exponents  $g(r) \sim r^{-2\tilde{\Delta}_\Phi}$ .

*Chiral QSL.* Next, we demonstrate the generality of the self-consistent approach by considering perturbing the U(1) Dirac QSL with a scalar spin chirality (SSC) term [46]

$$\mathcal{H} = \mathcal{H}_{J_1 J_2} + J_\chi \sum_{ijk \in \Delta, \nabla} \vec{S}_i \cdot (\vec{S}_j \times \vec{S}_k), \quad (8)$$

where  $ijk$  is an ordered set of the three spins on each triangular plaquette. The SSC term induces six-fermion

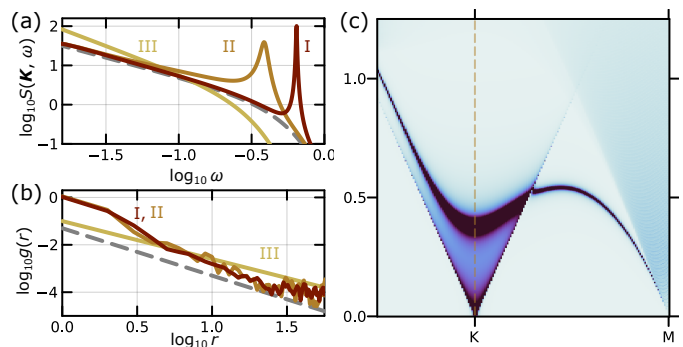


Figure 3. (a) Spectral weight at the  $\mathbf{K}$  point, including fermion and divergent gauge field contributions. Evaluated at three points of the phase diagram I–III within different approximation schemes. I:  $J_2 = J_1/8$  with independent gauge and fermion sectors; II:  $J_2 = 0.09J_1$  in the perturbative coupling approximation; III:  $J_2 = J_{2,c}$ , with a scaling Ansatz. (b) Real-space spin-spin correlation function  $g(r)$  along the direction of nearest-neighbour bonds. (c) Momentum-resolved structure factor  $S(\mathbf{q}, \omega)$  in model II, showing hybridization of the paramagnon and monopoles. All energies in units of  $J_1$  and lengths in units of lattice constant  $a$ .

interactions; decoupling them in the mean-field channel induces a staggered phase in the mean-field state (3), shifting it from  $[\pi, 0]$  to  $[\pi - \phi, \phi]$ , with  $\phi \sim tJ_\chi/J_1$ . It breaks time-reversal symmetry and opens up a gap linear in  $J_\chi$  for the fermion bands, which acquire a non-zero Chern number. The effective four-fermion vertex that one must consider in the RPA scheme gets corrected at order  $(J_\chi/J_1)^2$ ; given that the SSC interaction couples fermions across a triangle, the coupling at this order induces an effective on-site, nearest- and next-nearest neighbour interaction (like Hubbard  $U$ , and  $J_{1,2}$  terms) which tend to lower the paramagnon mode across the whole BZ.

Fig. 4 displays the structure factor, which shows a gap opening at the  $\mathbf{M}$  point and a sharp mode forming below the continuum there. For larger  $J_\chi$ , the gap increases linearly and the mode gets pushed down quadratically in the coupling strength. For larger  $J_2/J_1 \approx 0.15$ , the dominant effect of the SSC coupling will be due to the effective increase in  $J_2$ . In the absence of time reversal symmetry, this acts to condense the mode at  $\mathbf{M}$  destabilizing the chiral QSL towards tetrahedral order [47, 48]. For lower  $J_2/J_1 \sim 0.09$  the dominant contribution of SSC will be due to the effective  $J_1/U$  which try to condense the mode minimum at  $\mathbf{K}$  [49]. Overall, there can be a stable region of the gapped chiral QSL for small  $J_\chi$  and the condensation of the mode predicts instabilities to non-coplanar ordered phases.

*Outlook.* We used a self-consistent parton MFT+RPA theory to study the dynamical response and stability of the U(1) QSL on the triangular lattice for realistic spin Hamiltonians. We find that interactions be-

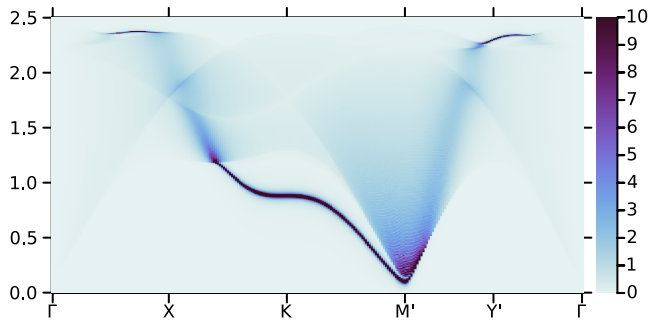


Figure 4. Structure factor for the chiral QSL phase  $S(\mathbf{q}, \omega)$ . We take  $J_2 = 1/8$  and  $J_\chi > 0$ . All energies  $\omega$  and interactions  $J_2, J_\chi$  in units of  $J_1$ .

tween spinons lead to sharp spinon-exciton bound states which dominate the spectral function over a large part of the finite-frequency response and interact with the broad spinon continuum in agreement with recent VMC [15] and tDMRG results [16, 17]. From condensation of the sharp modes we can deduce the stability of the QSL phases and neighboring ordered phases. The resulting phase diagram is in remarkable agreement with heavy-duty numerical methods. Overall, this points to a general applicability of our self-consistent method, which does not have any free parameters; i.e., if a parton MFT Ansatz is a good variational state, the RPA approach is a simple yet powerful tool for describing the dynamical response and stability of the QSL phase. We note, this success is corroborated by a complementary study investigating the  $Z_2$  Kitaev QSLs [50].

In light of recent evidence for (almost) gapless QSL-like response in triangular lattice magnets, i.e.  $\text{YbZn}_2\text{GaO}_5$  [51] and in the Yb-delafossites [52, 53], we also hope our method will allow a concrete comparison to INS experiments in order to pin down microscopic Hamiltonians. To this end, one can include spin anisotropy, interlayer coupling, or even disorder in our method for a quantitative description of candidate materials.

Open theoretical questions remain: First and foremost, it is unclear why the simple RPA works so well in describing the spin structure factor and stability of QSLs, particularly given that the  $U(1)$  states are expected to have strong gauge fluctuations. The unreasonable effectiveness of the RPA in this context is yet another example of the successful application of a theory beyond its original development context [54]. We introduced a phenomenological understanding of the low-energy physics of the  $U(1)$  Dirac QSL by describing the monopoles and spinons as independent particles that are perturbatively coupled, but a deeper understanding of the physics is a formidable open challenge. Second, beyond extending the self-consistent approach to other models, we think a great insight could be gained by calculating other dynamical correlation functions, for example the dynamical

dimer-dimer correlator. Numerical results of the  $U(1)$  DSL show that static dimer-dimer correlations are dominated by monopoles [55] and the role of spinon contributions at finite frequency is yet to be determined. We hope that it would also account for the QSL to valence bond solid (VBS) transition seen in the square-lattice  $J_1$ - $J_2$  model [56]. Furthermore, this response function would have predictive power for probes like resonant inelastic X-ray and Raman scattering.

*Acknowledgments.* We would like to thank F. Becca, M. Drescher, F. Ferrari, HuiKe Jin, M. Knap, F. Pollmann, P. Rao, U.F.P. Seifert and O.A. Starykh for insightful discussions. We thank A. Scheie and A. Tenant for helpful discussions regarding the experimental relevance of our work. We furthermore thank F. Becca and F. Ferrari for allowing us to reproduce data from Ref. [15]. J.K. also thanks for the hospitality of the Aspen Center for Physics, which is supported by National Science Foundation grant PHY-2210452. J.K. acknowledges support from the Deutsche Forschungsgemeinschaft (DFG, German Research Foundation) under Germany's Excellence Strategy (EXC-2111-390814868 and ct.qmat EXC-2147-390858490), and DFG Grants No. KN1254/1-2, KN1254/2-1 TRR 360 - 492547816 and SFB 1143 (project-id 247310070), as well as the Munich Quantum Valley, which is supported by the Bavarian state government with funds from the Hightech Agenda Bayern Plus. J.K. further acknowledges support from the Imperial-TUM flagship partnership.

---

\* joe.willsher@tum.de

- [1] X.-G. Wen, *Quantum field theory of many-body systems: From the origin of sound to an origin of light and electrons* (Oxford university press, 2004).
- [2] E. Fradkin, *Field theories of condensed matter physics* (Cambridge University Press, 2013).
- [3] L. Savary and L. Balents, Quantum spin liquids: A review, *Reports on Progress in Physics* **80**, 016502 (2016).
- [4] J. Knolle and R. Moessner, A Field Guide to Spin Liquids, *Annual Review of Condensed Matter Physics* **10**, 451 (2019).
- [5] A. Kitaev, Anyons in an exactly solved model and beyond, *Annals of Physics* **321**, 2 (2006).
- [6] G. Baskaran, Z. Zou, and P. W. Anderson, The resonating valence bond state and high- $T_c$  superconductivity—a mean field theory, *Solid state communications* **88**, 853 (1993).
- [7] X.-G. Wen, Quantum orders and symmetric spin liquids, *Physical Review B* **65**, 165113 (2002).
- [8] Th. Jolicoeur, E. Dagotto, E. Gagliano, and S. Bacci, Ground-state properties of the  $S=1/2$  Heisenberg antiferromagnet on a triangular lattice, *Physical Review B*

- 42**, 4800 (1990).
- [9] A. V. Chubukov and Th. Jolicoeur, Order-from-disorder phenomena in Heisenberg antiferromagnets on a triangular lattice, *Physical Review B* **46**, 11137 (1992).
- [10] R. Kaneko, S. Morita, and M. Imada, Gapless spin-liquid phase in an extended spin 1/2 triangular heisenberg model, *Journal of the Physical Society of Japan* **83**, 093707 (2014), <https://doi.org/10.7566/JPSJ.83.093707>.
- [11] W.-J. Hu, S.-S. Gong, W. Zhu, and D. N. Sheng, Competing spin-liquid states in the spin- $\frac{1}{2}$  Heisenberg model on the triangular lattice, *Physical Review B* **92**, 140403 (2015).
- [12] Z. Zhu and S. R. White, Spin liquid phase of the  $S=\frac{1}{2}$   $J_1$ - $J_2$  Heisenberg model on the triangular lattice, *Physical Review B* **92**, 041105 (2015).
- [13] Y. Iqbal, W.-J. Hu, R. Thomale, D. Poilblanc, and F. Becca, Spin liquid nature in the Heisenberg  $J_1$ - $J_2$  triangular antiferromagnet, *Physical Review B* **93**, 144411 (2016).
- [14] S. Hu, W. Zhu, S. Eggert, and Y.-C. He, Dirac spin liquid on the spin-1/2 triangular heisenberg antiferromagnet, *Physical Review Letters* **123**, 207203 (2019).
- [15] F. Ferrari and F. Becca, Dynamical structure factor of the  $J_1 - J_2$  heisenberg model on the triangular lattice: Magnons, spinons, and gauge fields, *Physical Review X* **9**, 031026 (2019).
- [16] M. Drescher, L. Vanderstraeten, R. Moessner, and F. Pollmann, Dynamical signatures of symmetry-broken and liquid phases in an  $S = 1/2$  Heisenberg antiferromagnet on the triangular lattice, *Physical Review B* **108**, L220401 (2023).
- [17] N. E. Sherman, M. Dupont, and J. E. Moore, Spectral function of the  $j_1$ - $j_2$  heisenberg model on the triangular lattice, *Physical Review B* **107**, 165146 (2023).
- [18] M. Hermele, T. Senthil, and M. P. Fisher, Algebraic spin liquid as the mother of many competing orders, *Physical Review B—Condensed Matter and Materials Physics* **72**, 104404 (2005).
- [19] X.-Y. Song, C. Wang, A. Vishwanath, and Y.-C. He, Unifying description of competing orders in two-dimensional quantum magnets, *Nature Communications* **10**, 4254 (2019).
- [20] X.-Y. Song, Y.-C. He, A. Vishwanath, and C. Wang, From Spinon Band Topology to the Symmetry Quantum Numbers of Monopoles in Dirac Spin Liquids, *Physical Review X* **10**, 011033 (2020).
- [21] M. Hermele, Y. Ran, P. A. Lee, and X.-G. Wen, Properties of an algebraic spin liquid on the kagome lattice, *Physical Review B* **77**, 224413 (2008).
- [22] U. F. P. Seifert, J. Willsher, M. Drescher, F. Pollmann, and J. Knolle, Spin-Peierls instability of the U(1) Dirac spin liquid, *Nature Communications* **15**, 7110 (2024).
- [23] Formally these are fluctuations of the Hubbard–Stratonovich saddle points of the mean-field order. We develop a Landau–Ginzburg theory in the End Matter.
- [24] J. R. Schrieffer, X. G. Wen, and S. C. Zhang, Dynamic spin fluctuations and the bag mechanism of high- $T_c$  superconductivity, *Physical Review B* **39**, 11663 (1989).
- [25] A. V. Chubukov and D. M. Frenkel, Renormalized perturbation theory of magnetic instabilities in the two-dimensional Hubbard model at small doping, *Physical Review B* **46**, 11884 (1992).
- [26] A. P. Kampf, Collective excitations in itinerant spiral magnets, *Physical Review B* **53**, 747 (1996).
- [27] N. Peres and M. Araújo, Spin-wave dispersion in  $la_2cuo_4$ , *Physical Review B* **65**, 132404 (2002).
- [28] A. Singh, Finite  $U$ -induced competing interactions, frustration, and quantum phase transition in a triangular-lattice antiferromagnet, *Physical Review B* **71**, 214406 (2005).
- [29] J. Knolle, I. Eremin, A. V. Chubukov, and R. Moessner, Theory of itinerant magnetic excitations in the spin-density-wave phase of iron-based superconductors, *Physical Review B* **81**, 140506 (2010).
- [30] J. Knolle, I. Eremin, and R. Moessner, Multiorbital spin susceptibility in a magnetically ordered state: Orbital versus excitonic spin density wave scenario, *Physical Review B—Condensed Matter and Materials Physics* **83**, 224503 (2011).
- [31] J. Willsher, H.-K. Jin, and J. Knolle, Magnetic excitations, phase diagram, and order-by-disorder in the extended triangular-lattice Hubbard model, *Physical Review B* **107**, 064425 (2023).
- [32] C.-M. Ho, V. N. Muthukumar, M. Ogata, and P. W. Anderson, Nature of Spin Excitations in Two-Dimensional Mott Insulators: Undoped Cuprates and Other Materials, *Physical Review Letters* **86**, 1626 (2001).
- [33] N. Ma, G.-Y. Sun, Y.-Z. You, C. Xu, A. Vishwanath, A. W. Sandvik, and Z. Y. Meng, Dynamical signature of fractionalization at a deconfined quantum critical point, *Physical Review B* **98**, 174421 (2018).
- [34] L. Balents and O. A. Starykh, Collective spinon spin wave in a magnetized U(1) spin liquid, *Physical Review B* **101**, 020401 (2020).
- [35] Y. Zhou and X.-G. Wen, *Quantum Orders and Spin Liquids in  $Cs_2CuCl_4$*  (2003), [arXiv:cond-mat/0210662](https://arxiv.org/abs/cond-mat/0210662).
- [36] E. A. Ghioldi, M. G. Gonzalez, S.-S. Zhang, Y. Kamiya, L. O. Manuel, A. E. Trumper, and C. D. Batista, Dynamical structure factor of the triangular antiferromagnet: Schwinger boson theory beyond mean field, *Physical Review B* **98**, 184403 (2018).
- [37] C. Zhang and T. Li, Resonating valence bond theory of anomalous spin dynamics of spin-1/2 triangular lattice Heisenberg antiferromagnet and its application to  $Ba_3CoSb_2O_9$ , *Physical Review B* **102**, 075108 (2020).
- [38] T. Appelquist, D. Nash, and L. C. R. Wijewardhana, Critical behavior in (2+1)-dimensional QED, *Physical Review Letters* **60**, 2575 (1988).
- [39] T. Grover, Entanglement monotonicity and the stability of gauge theories in three spacetime dimensions, *Physical Review Letters* **112**, 151601 (2014).
- [40] A. Wietek, S. Capponi, and A. M. Läuchli, Quantum Electrodynamics in 2 + 1 Dimensions as the Organizing Principle of a Triangular Lattice Antiferromagnet, *Physical Review X* **14**, 021010 (2024).
- [41] S. Budaraju, A. Parola, Y. Iqbal, F. Becca, and D. Poilblanc, *Monopole excitations in the  $U(1)$  Dirac spin liquid on the triangular lattice* (2024), [arXiv:2410.18747](https://arxiv.org/abs/2410.18747).
- [42] L. D. Pietro and E. Stamou, Scaling dimensions in QED3 from the  $\epsilon$ -expansion, *Journal of High Energy Physics* **2017**, 10.1007/jhep12(2017)054 (2017).
- [43] É. Dupuis, M. B. Paranjape, and W. Witczak-Krempa, Transition from a Dirac spin liquid to an antiferromagnet: Monopoles in a QED 3 -Gross-Neveu theory, *Physical Review B* **100**, 094443 (2019).

- [44] S. Albayrak, R. S. Erramilli, Z. Li, D. Poland, and Y. Xin, Bootstrapping  $N_f=4$  conformal QED<sub>3</sub>, *Physical Review D: Particles and Fields* **105**, 085008 (2022).
- [45] Justified by the separation in scales, detailed in the Supplementary Materials. As the spectral weight of the monopole diverges as  $m \rightarrow 0$ , this approximation breaks down.
- [46] W.-J. Hu, S.-S. Gong, and D. Sheng, Variational monte carlo study of chiral spin liquid in quantum antiferromagnet on the triangular lattice, *Physical Review B* **94**, 075131 (2016).
- [47] A. Wietek and A. M. Läuchli, Chiral spin liquid and quantum criticality in extended  $S = 1/2$  Heisenberg models on the triangular lattice, *Physical Review B* **95**, 035141 (2017).
- [48] T. Cookmeyer, J. Motruk, and J. E. Moore, Four-spin terms and the origin of the chiral spin liquid in mott insulators on the triangular lattice, *Physical review letters* **127**, 087201 (2021).
- [49] F. Pichler, W. Kadow, C. Kuhlenkamp, and M. Knap, Probing magnetism in moiré heterostructures with quantum twisting microscopes, *Phys. Rev. B* **110**, 045116 (2024).
- [50] P. Rao, R. Moessner, and J. Knolle, *Dynamical response theory of interacting majorana fermions and its application to generic kitaev quantum spin liquids in a field* (2025), arXiv:2503.10330 [cond-mat.str-el].
- [51] R. Bag, S. Xu, N. E. Sherman, L. Yadav, A. I. Kolesnikov, A. A. Podlesnyak, E. S. Choi, I. Da Silva, J. E. Moore, and S. Haravifard, Evidence of dirac quantum spin liquid in ybzn 2 gao 5, *Physical Review Letters* **133**, 266703 (2024).
- [52] A. Scheie, E. Ghioldi, J. Xing, J. Paddison, N. Sherman, M. Dupont, L. Sanjeeva, S. Lee, A. Woods, D. Abernathy, *et al.*, Proximate spin liquid and fractionalization in the triangular antiferromagnet kybse2, *Nature Physics* **20**, 74 (2024).
- [53] A. O. Scheie, M. Lee, K. Wang, P. Laurell, E. S. Choi, D. Pajerowski, Q. Zhang, J. Ma, H. D. Zhou, S. Lee, S. M. Thomas, M. O. Ajeesh, P. F. S. Rosa, A. Chen, V. S. Zapf, M. Heyl, C. D. Batista, E. Dagotto, J. E. Moore, and D. A. Tennant, *Spectrum and low-energy gap in triangular quantum spin liquid NaYbSe<sub>2</sub>* (2024), arxiv:2406.17773 [cond-mat].
- [54] E. P. Wigner, The unreasonable effectiveness of mathematics in the natural sciences, in *Mathematics and science* (World Scientific, 1990) pp. 291–306.
- [55] F. Ferrari, J. Willsher, U. F. P. Seifert, R. Valentí, and J. Knolle, *Stability of algebraic spin liquids coupled to quantum phonons* (2024), arXiv:2410.16376.
- [56] S. Morita, R. Kaneko, and M. Imada, Quantum spin liquid in spin 1/2 j<sub>1</sub>-j<sub>2</sub> heisenberg model on square lattice: Many-variable variational monte carlo study combined with quantum-number projections, *journal of the physical society of japan* **84**, 024720 (2015).
- [57] Z. Y. Weng, C. S. Ting, and T. K. Lee, Path-integral approach to the Hubbard model, *Physical Review B* **43**, 3790 (1991).

## End Matter

### Mean field Hamiltonian

The pi-flux Ansatz and its two-site unit cell is drawn in Fig. 5(a). The fermion hopping in real space is chosen to be  $\pm t$  on the black/blue bonds. We construct our theory in terms of sublattice fermions  $f_{i,X}$  where  $X = A, B$ . The lattice unit vectors are  $\mathbf{a}_1 = (2, 0)$ ,  $\mathbf{a}_2 = (1/2, \sqrt{3}/2)$ . Consequently, the reciprocal space is shown in Fig. 5(b); the inverse lattice unit vectors are  $\mathbf{q}_1 = \pi/a(1, -1/\sqrt{3})$  and  $\mathbf{q}_2 = (0, 4\pi/a\sqrt{3})$ . We henceforth use a basis of momenta  $\mathbf{k} = k_1\mathbf{Q}_1 + k_2\mathbf{Q}_2$  and the reduced Brillouin zone is drawn as the gray dashed rectangle.

The Hamiltonian (which is diagonal in spin) can be written in terms of a spinor  $\Psi_{\mathbf{k},m}$

$$\mathcal{H}_0 = \sum_{\mathbf{k}} \Psi_{\mathbf{k}}^\dagger H(\mathbf{k}) \Psi_{\mathbf{k}} \quad (9)$$

with combined spin-sublattice index  $m = (\alpha, X)$ . The spinor components are explicitly  $\Psi_{\mathbf{k}} = (f_{\mathbf{k}\uparrow,A}, f_{\mathbf{k}\downarrow,A}, f_{\mathbf{k}\uparrow,B}, f_{\mathbf{k}\downarrow,B})^T$  and the Bloch Hamiltonian in this basis is

$$H_{\alpha\beta}^{XY}(\mathbf{k}) = J_1 t \delta_{\alpha\beta} M_{\mathbf{k}}^{XY} \quad (10)$$

where explicitly the phases are given by

$$\begin{aligned} M_{\mathbf{k}}^{AA} &= -M_{\mathbf{k}}^{BB} = 2 \cos(k_2) \\ M_{\mathbf{k}}^{AB} &= 1 + e^{-ik_1} + e^{i(k_2-k_1)} - e^{-ik_2}, \end{aligned} \quad (11)$$

and where  $M_{\mathbf{k}}^{XY} = (M_{\mathbf{k}}^{YX})^*$ . The eigenvalues of this matrix  $H_{mn}(\mathbf{k})$  are written  $\varepsilon_{\mathbf{k}}^m$  with corresponding eigenvectors  $\alpha_{\mathbf{k}}^m$ . The overall normalisation of this mean-field Hamiltonian is fixed self-consistently by evaluating  $t = \frac{J_1}{N} \sum_{\mathbf{k}\alpha} \langle f_{\mathbf{k}\alpha,A}^\dagger f_{\mathbf{k}\alpha,B} \rangle$ .

### Susceptibility

The contribution of the spinons to the structure factor (4) can be formulated by explicitly decomposing the spins

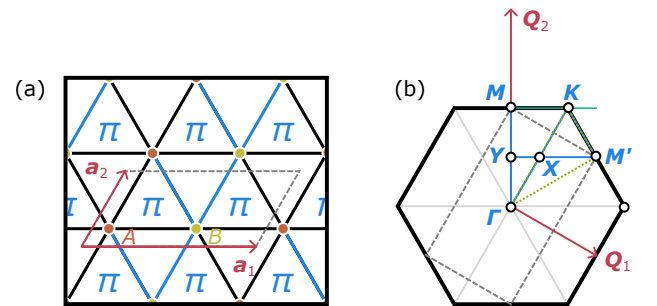


Figure 5. (a) Pi flux Ansatz with  $A, B$  sites within the unit cell highlighted. Lattice vectors  $\mathbf{a}_{1,2}$  and reciprocal lattice unit vectors  $\mathbf{Q}_{1,2}$  highlighted.w

into Fourier-space fermions in the sublattice basis. We write it as a sum over the susceptibility matrix

$$S(\mathbf{q}, \omega) = \text{Im} \sum_{X,Y=A,B} e^{-i\mathbf{q}\cdot(\mathbf{r}_X - \mathbf{r}_Y)} [\chi(\mathbf{q}, \omega)]_{XY}^{zz}, \quad (12)$$

$$[\chi(\mathbf{q}, \omega)]_{XY}^{ij} = \frac{i}{N} \int dt e^{i\omega t} \langle S_{X,\mathbf{q}}^i(t) S_{Y,-\mathbf{q}}^j(0) \rangle. \quad (13)$$

In terms of sublattice fermions in momentum space

$$[\chi(\mathbf{q}, \omega)]_{XY}^{ij} = \frac{i}{N} \int dt e^{i\omega t} \sum_{\mathbf{k}, \mathbf{k}'} \frac{1}{4} (\sigma^i)_{\alpha\beta} (\sigma^j)_{\gamma\delta} \times \langle T [f_{\alpha X, \mathbf{k}}^\dagger f_{\beta X, \mathbf{k}+\mathbf{q}}(t)] [f_{\gamma Y, \mathbf{k}'}^\dagger f_{\delta Y, \mathbf{k}'-\mathbf{q}}(0)] \rangle \quad (14)$$

Splitting into the single-particle interacting Green's functions

$$\mathcal{G}_{\alpha\beta}^{XY}(\mathbf{q}, t) = -\langle T f_{\alpha X, \mathbf{q}}(0) f_{\beta Y, \mathbf{q}}^\dagger(t) \rangle \quad (15)$$

and constraining  $\mathbf{k}' = \mathbf{k} + \mathbf{q}$ , we get

$$[\chi(\mathbf{q}, i\omega)]_{XY}^{ij} = -\frac{i}{4N} \sum_{\mathbf{k}, i\nu} (\sigma^i)_{\alpha\beta} (\sigma^j)_{\gamma\delta} \mathcal{G}_{\delta\alpha}^{YX}(\mathbf{k}, i\omega) \mathcal{G}_{\beta\gamma}^{XY}(\mathbf{k} + \mathbf{q}, i\omega + i\nu). \quad (16)$$

We combine the matrix elements and write them in terms of a combined index  $\mu = (i, X)$ . A Matsubara summation over the free fermion Green's functions gives the free susceptibility

$$[\chi^0(\mathbf{q}, \omega)]^{\mu\nu} = -\frac{i}{4N} \sum_{\mathbf{k}, mn} \frac{(n_{\mathbf{k}}^m - n_{\mathbf{k}+\mathbf{q}}^n) \mathcal{V}_{\mu}^{mn} (\mathcal{V}_{\nu}^{mn})^*}{\omega + \varepsilon_{\mathbf{k}}^m - \varepsilon_{\mathbf{k}+\mathbf{q}}^n} \quad (17)$$

where the Fermi-Dirac occupancies are  $n_{\mathbf{k}}^m = n_f(\varepsilon_{\mathbf{k}}^m)$  and the matrix elements defined as

$$\mathcal{V}_{\mu}^{mn} = (\alpha_{\mathbf{k}}^m)_{\alpha X}^* (\sigma^i)_{\alpha\beta} (\alpha_{\mathbf{k}+\mathbf{q}}^n)_{\beta X}. \quad (18)$$

The free fermion structure factor is plotted in Fig. 6.

### Random phase approximation

Transforming the interaction Eq. (1) into the sublattice Fourier basis, we express it as

$$\sum_{\mathbf{q}} \delta_{ij} J_{\mathbf{q}}^{XY} S_{X,\mathbf{q}}^i S_{Y,-\mathbf{q}}^j = \sum_{\mathbf{k}, \mathbf{k}', \mathbf{q}} \delta_{ij} J_{\mathbf{q}}^{XY} \frac{1}{4} \sigma_{\alpha\beta}^i \sigma_{\gamma\delta}^j \times \left( f_{\alpha X, \mathbf{k}+\mathbf{q}}^\dagger f_{\beta X, \mathbf{k}} \right) \left( f_{\gamma Y, \mathbf{k}'-\mathbf{q}}^\dagger f_{\delta Y, \mathbf{k}'} \right). \quad (19)$$

The Fourier interaction strength in the sublattice basis is explicitly given by

$$\begin{aligned} J_{\mathbf{q}}^{XX} &= J_{\mathbf{q}}^{YY} = 2J_1 \cos(k_2) + 2J_2 \cos(k_1 - k_2) \\ J_{\mathbf{q}}^{XY} &= J_1 \left[ 1 + e^{-ik_1} + e^{i(k_2 - k_1)} + e^{-ik_2} \right] \\ &\quad + J_2 \left[ e^{ik_2} + e^{i(2k_2 - k_1)} + e^{-i(k_1 + k_2)} + e^{-2ik_2} \right] \end{aligned} \quad (20)$$

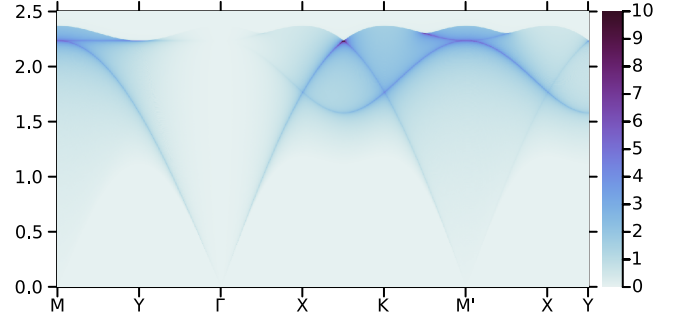


Figure 6. Fermion contribution to the dynamical structure factor  $S(\mathbf{q}, \omega)$  in the free fermion (zeroth order mean-field) approximation,  $[\chi^0(\mathbf{q}, \omega)]$ . We neglect the strong fermion-fermion interactions here. All energies  $\omega$  in units of  $J_1$ .

and where  $J_{\mathbf{q}}^{XY} = (J_{\mathbf{q}}^{YX})^*$ . Note that these elements  $J^{XY}$  differ from the Hamiltonian (11) since the signs do not alternate on different bonds in the unit cell, and there is no self-consistent amplitude  $t$ , which is only non-zero on nearest-neighbor bonds in  $M^{XY}$ . Importantly, this means that next-nearest neighbor interactions are non-zero and will modify the physics of the model beyond the self-consistent mean-field approximation.

The effect of the interaction on the spin susceptibility can be accounted for by resumming a series of bubble diagrams. The interacting spin susceptibility can be written in terms of the bare susceptibility as follows

$$[\chi(\mathbf{q}, \omega)]^{\mu\nu} = [\chi^0(\mathbf{q}, \omega)]^{\mu\nu} + [\chi^0(\mathbf{q}, \omega)]^{\mu\rho} J_{\mathbf{q}}^{\rho\sigma} [\chi(\mathbf{q}, \omega)]^{\sigma\nu}. \quad (21)$$

A perturbative calculation in the Supplementary Materials finds that the interaction matrix in this basis is given by  $J_{\mathbf{q}}^{\mu\nu} = -2\delta_{ij} J_{\mathbf{q}}^{XY}$ . It is manifestly diagonal in spin indices. Since the spin liquid state has SU(2) spin symmetry, the free susceptibility is also diagonal  $[\chi(\mathbf{q}, \omega)]_{XY}^{ij} = \delta^{ij} [\hat{\chi}(\mathbf{q}, \omega)]_{XY}$ , which allows us to ignore transverse fluctuations and calculate everything in terms of the longitudinal susceptibility matrix. The Dyson equation (21) can be inverted and solved in the sublattice basis to find

$$\hat{\chi}(\mathbf{q}, \omega) = \left[ 1 + 2\hat{J}_{\mathbf{q}} \cdot \hat{\chi}^0(\mathbf{q}, \omega) \right]^{-1} \cdot \hat{\chi}^0(\mathbf{q}, \omega), \quad (22)$$

as Eq. (6). We present a comparison to the VMC results from Ref. [15] in Fig. 7, showing very good agreement.

### Stability

We want to derive the condition for the stability of a mean-field QSL ground state of a magnetic Hamiltonian (1). Following Ref. [57], we can formulate the interacting theory in the path-integral formulation, considering the fluctuations of the mean-field amplitude  $t = J_1 \chi$ , ‘charge’ ordering  $\rho$ , and spin ordering  $\vec{m}$ . We perform a series of

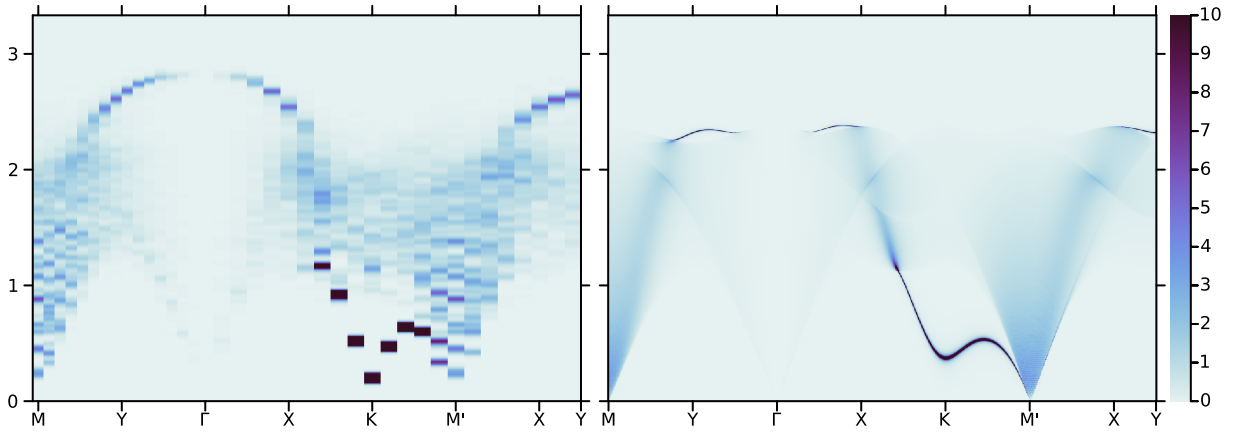


Figure 7. Fermion contribution to the dynamical structure factor  $S(\mathbf{q}, \omega)$  in the random phase approximation (right) and from Ref. [15] (left). We take  $J_2/J_1 = 0.09$  in the U(1) Dirac QSL phase; all energies  $\omega$  in units of  $J_1$ .

Hubbard–Stratonovich decouplings of (1) to give

$$\mathcal{H} = \sum_{ij} J_{ij} \left[ \frac{1}{2} \left( \chi_{ij} f_j^\dagger f_i + \text{h.c.} - |\chi_{ij}|^2 \right) + \left( \vec{m}_i \cdot \vec{m}_j - 2\vec{m}_i \cdot (f_j^\dagger \vec{\sigma} f_j) \right) \right] + i\lambda (f_i^\dagger f_i - 1). \quad (23)$$

A mean-field theory of a magnetically ordered state is described by a saddle point of (23) with  $m_i^\alpha = \frac{1}{2} \langle f_i^\dagger \sigma_\alpha f_i \rangle \neq 0$  and  $\chi_{ij} = 0$ . The excitations are gapless Goldstone modes and gapped amplitude fluctuations of  $m_i$  and  $\chi_{ij}$  [57]. A mean-field theory of a QSL-ordered state is instead described by another saddle point  $\chi_{ij} = 2 \langle f_i^\dagger f_j \rangle \neq 0$  with  $m_i^\alpha = 0$ , giving (3). The bosonic excitations are gapped amplitude fluctuations of  $m_i$  and  $\chi_{ij}$ , as

well as the gapless phase fluctuations of  $\chi_{ij}$ . We derive the effective action of the gapped bosonic spin-singlet  $\delta\chi_{ij} = |\chi_{ij}| - 2|\langle f_i^\dagger f_j \rangle|$  and magnetic ordering amplitude fluctuations  $m_i$ , in the one-loop approximation as

$$\mathcal{L}[m_q] = \frac{1}{2} [J_q^{-1} - \Pi_q^0 + \dots] m_q m_{-q}, \quad (24)$$

where  $\Pi_q^0 = \text{Re} \chi^0(\mathbf{q}, 0)$ . This leads to a magnetic ordering instability when  $[1 - J_q \Pi_q^0(\mathbf{q}, 0)] = 0$ . This softening of the spin-stiffness to order at wavevector  $\mathbf{q}$  coincides with the RPA pole condition of the collective mode at  $\omega = 0$ , derived in the Supplementary Materials. Equivalently, we predict that there will be an instability to spin-singlet (VBS) order when  $[J_q^{-1} - \tilde{\Pi}_q^0] = 0$ , where  $\tilde{\Pi}_q^0$  is an analogous zero-frequency limit of the dimer-dimer susceptibility.